




Article

# Decreased Expression of CIRP Induced by Therapeutic Hypothermia Correlates with Reduced Early Brain Injury after Subarachnoid Hemorrhage

Haibin Dai <sup>1,†</sup>, Yan Zhou <sup>1,†</sup>, Yue Lu <sup>1</sup>, Xiangsheng Zhang <sup>2</sup>, Zong Zhuang <sup>1</sup>, Yongyue Gao <sup>1</sup>, Guangjie Liu <sup>1</sup> , Chunlei Chen <sup>1</sup>, Jin Ma <sup>3,\*</sup>, Wei Li <sup>1</sup> and Chunhua Hang <sup>1,\*</sup>

<sup>1</sup> Department of Neurosurgery, Nanjing Drum Tower Hospital, Medical School of Nanjing University, Nanjing 210008, China; daisea2006@sina.com (H.D.); oatmeal0329@163.com (Y.Z.); njuluyue@163.com (Y.L.); zhuangzong@126.com (Z.Z.); tallergao@163.com (Y.G.); 15195880897@163.com (G.L.); 15720801655@163.com (C.C.); lwxzlw@126.com (W.L.)

<sup>2</sup> Department of Neurosurgery, Beijing Friendship Hospital, Capital Medical University, Beijing 100050, China; 15895971847@163.com

<sup>3</sup> Department of Medical Equipment, School of Aerospace Medicine, Air Force Medical University, Xi'an 710032, China

\* Correspondence: 780216@fmmu.edu.cn (J.M.); hang\_neurosurgery@163.com (C.H.); Tel.: +86-29-84774825 (J.M.); +86-25-83106666 (C.H.)

† These authors contributed equally to this work.



**Citation:** Dai, H.; Zhou, Y.; Lu, Y.; Zhang, X.; Zhuang, Z.; Gao, Y.; Liu, G.; Chen, C.; Ma, J.; Li, W.; et al. Decreased Expression of CIRP Induced by Therapeutic Hypothermia Correlates with Reduced Early Brain Injury after Subarachnoid Hemorrhage. *J. Clin. Med.* **2022**, *11*, 3411. <https://doi.org/10.3390/jcm11123411>

Academic Editors: Guoyi Gao and Lindsay A. Farrer

Received: 11 May 2022

Accepted: 11 June 2022

Published: 14 June 2022

**Publisher's Note:** MDPI stays neutral with regard to jurisdictional claims in published maps and institutional affiliations.



**Copyright:** © 2022 by the authors. Licensee MDPI, Basel, Switzerland. This article is an open access article distributed under the terms and conditions of the Creative Commons Attribution (CC BY) license (<https://creativecommons.org/licenses/by/4.0/>).

**Abstract:** Early brain injury is considered to be a primary reason for the poor prognosis of patients suffering from subarachnoid hemorrhage (SAH). Due to its pro-inflammatory activity, cold-inducible RNA-binding protein (CIRP) has been implicated in the ischemic brain insult, but its possible interplay with hypothermia in SAH treatment remains to be evaluated. One-hundred and thirty-eight Sprague-Dawley rats (300–350 g males) were randomly allocated into the following groups: sham-operated (Sham); SAH; and SAH + hypothermia (SAH + H), each comprised of 46 animals. After treatments, the brain tissues of the three groups were randomly collected after 12 h, 1 d, 3 d, and 7 d, and the expression levels of the CIRP and mitochondrial apoptosis pathway-related proteins Bax, Bcl-2, caspase-9, caspase-3, and cytochrome c measured using Western blotting and real-time PCR. Brain damage was assessed by TUNEL and Nissl staining, the electron microscopy of brain tissue slices as well as functional rotarod tests. Expression of CIRP, Bax, caspase-9, caspase-3, and cytochrome c as well as reduced motor function incidence were higher in the SAH group, particularly during the first 3 d after SAH induction. Hypothermia blunted these SAH responses and apoptosis, thereby indicating reduced inflammatory signaling and less brain cell injury in the early period after SAH. Hypothermia treatment was found to effectively protect the brain tissue from early SAH injury in a rat model and its further evaluation as a therapeutic modality in SAH patients requires further study.

**Keywords:** subarachnoid hemorrhage (SAH); cold-inducible RNA-binding protein (CIRP); hypothermia; early brain injury; apoptosis

## 1. Introduction

Subarachnoid hemorrhage (SAH), typically caused by the spontaneous rupture of an intracranial aneurysm, is a life-threatening condition associated with a high rate of disability and mortality [1]. Traditionally, vasospasm after SAH was considered to be the most decisive determinant of brain damage and poor prognosis for patients [2]. However, recent findings have suggested that damage to the brain cells (neurons and glial cells) usually occurs early after SAH (within 10 min) [3]. Thus, brain injury during the early stage may be the main reason for poor prognosis in patients who have had a SAH [4,5]. Similarly, one of the reasons for the response times of patients with ischemic stroke has been patient perception of early symptoms as being severe or very severe [6].

Cold-inducible RNA-binding protein (CIRP) is an RNA binding protein that is extensively expressed in the cerebral cortex [7,8], and is a member of a family of highly conserved cold shock proteins that are continuously expressed at low levels in mammalian cells [9–11]. CIRP affects mRNA transcription and translation and facilitates a rapid response to environmental changes at the cellular level. Moreover, CIRP may act as a molecular chaperone to assist in the folding and assembly/disassembly of DNA structures as well as a role in intracellular protein transport [10,12].

CIRP has been shown to mediate neuro-inflammation in cerebral ischemia, hemorrhagic shock, and other diseases [13,14]. In addition, CIRP also modulates inflammatory responses by several distinct mechanisms including binding to the TLR4-MD2 complex to act as a damage-associated molecular pattern, activating the NF- $\kappa$ B pathway, and stimulating the production of pro-inflammatory cytokines [15].

Therapeutic hypothermia is considered as an emerging option for the treatment of SAH [16] and a meta-analysis of animal studies revealed multiple indications of the beneficial effects of hypothermia, especially when applied shortly after temporary ischemia [17]. It is thought that reduced energy consumption due to the inhibition of intracellular signaling pathways such as calcium movements that prevent the depletion of ATP and the generation of free radicals underlie the protective effects of hypothermia [18]. Hypothermia also modulates the inflammatory and apoptotic signaling pathways, leading to a decrease in the secretion of excitatory neurotransmitters and blunted inflammatory responses [19]. Since ischemic or hemorrhagic stroke and SAH are underlying causes of status epilepticus, hypothermia, combined with standard therapy, has been applied to improve the neurological outcomes in patients with convulsive status epilepticus. However, hypothermia had no significant effect on 90 d outcomes in the HYBERNATUS clinical trial [20], but did reduce the rate of progression to d-1 EEG-confirmed status epilepticus. Despite these research efforts, the possible interplay of hypothermia with CIRP expression and neuronal apoptosis has remained largely unexplored.

A vital checkpoint in the apoptosis pathway is the ratio of pro-apoptotic (Bax) to anti-apoptotic (Bcl-2) BH domain proteins. Downstream, two mechanisms that are likely to be involved in SAH-induced neuronal cell death are caspase activation and mitochondrial dysfunction, as indicated by the increased cytoplasmic cytochrome c levels [21].

In the present study, an SAH model in the rat chiasmatic cistern was established. The expression levels of CIRP, Bax, Bcl-2, caspase-9, caspase-3, and cytochrome c in the treatment and control groups were quantified to explore the effects of hypothermia treatment on the degree of induction of CIRP in the rat brain tissue and its correlation to the recovery from early brain damage. Based on previous findings, we hypothesized that CIRP may play a hitherto unexplored role in the early stages of brain damage caused by SAH and also focused on apoptosis related markers.

## 2. Materials and Methods

### 2.1. Animals

One-hundred and thirty-eight Sprague-Dawley rats (300–350 g, only male rats were chosen to avoid possible gender differences) were used in the experiments. To adapt to the environment, rats were housed for 1 week prior to the experiments under standard husbandry conditions as follows: room temperature 22 to 25 °C; 12-h light/dark cycle; relative humidity 50–60%; access to standard chow and water ad libitum. Twelve hours prior to an experiment, food was withheld but free access to water was granted. All experimental procedures were approved by the Animal Care and Use Committee of Nanjing University and were performed in accordance with the Guidelines for the Humane Treatment of Laboratory Animals (Ministry of Science and Technology of the People's Republic of China, Policy No. 2006398).

### 2.2. Injection of Blood into the Chiasmatic Cistern-SAH Model

The SAH model has been previously described but used here with minor modifications [22]. In brief, after being deeply anesthetized with i.p. 10% chloral hydrate (0.35 mL per 100 g), the rat femoral artery viewed under a microscope (MM500-N; Leica Microsystems Ltd., Wetzlar, Germany) was dissected to extract autologous arterial blood. A hole was drilled 8 mm in front of the anterior fontanelle in the midline of the skull. The chiasmatic cistern was located with the assistance of a stereo locator (RWD Life Science Co., Ltd., Shenzhen, China). A 1 mL insulin injection needle was inserted into the hole about 10 mm deep at an angle of 30° to reach the chiasmatic cistern. Five-hundred µL of autologous arterial blood was injected through an aseptic injection pump over a time period of 20 s. The hole in the skull was sealed with bone wax, followed by suturing of the scalp. The same volume of saline was injected into the chiasmatic cistern of the sham-operated (Sham) group. All treatments were performed in a dedicated laboratory space.

### 2.3. Experimental Groups

Rats were first numbered and then without the confounder control divided into three groups according to a random number table: (1) Sham-operation (Sham,  $n = 46$ ); (2) SAH ( $n = 46$ ); and (3) SAH + hypothermia (SAH + H,  $n = 46$ ) (Figure 1). The principle of random assignment was still followed when sacrificing the rats and performing the histological examinations. The SAH + H group underwent surface cooling, using an ice bag immediately after the model was established, as previously described [23]. The rectal temperature was decreased to 30–31 °C within 30 min and maintained for 6 h by adjusting the distance of the ice bag from the animal. The rectal temperature in the other two groups was maintained at 36–37 °C. When the anesthetic effect wore off, rats in the Sham and SAH groups awoke after ~2 h and moved their limbs and heads. If there were signs of awakening during the 6 h of hypothermia treatment in the SAH + H group, 50% of the original dose of chloral hydrate was injected i.p. After 6 h of hypothermia treatment, animals were kept warm until awakening. No rat in the Sham group died, but five rats died in the SAH + H group during hypothermia treatment (10.8% mortality) and in the SAH group, six rats died (13% mortality). All dead rats were excluded from further analyses.

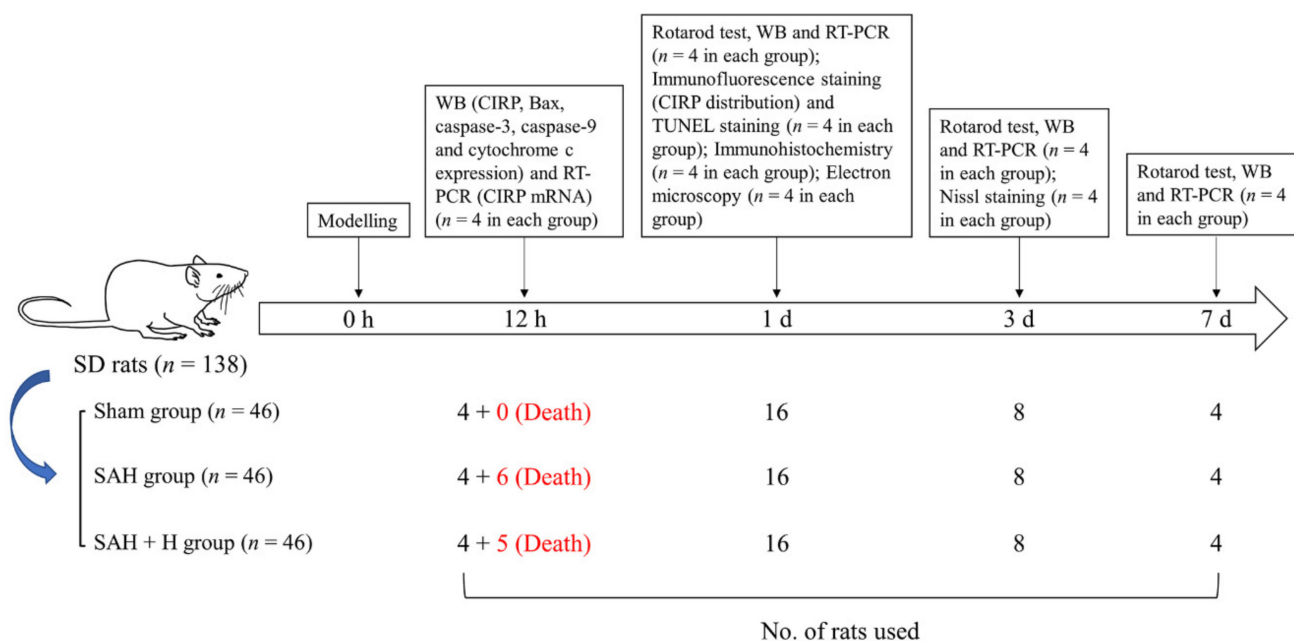


Figure 1. The schematic illustration of the experimental workflow.

#### 2.4. Acquisition of Brain Tissue after SAH

In this study, *n* refers to the number of animals per group, with two brain tissues obtained from each experimental animal (bilateral temporal lobe cortex) at each time point, which were then used for further analyses. To capture the early as well as long-term effects, brain specimens were collected at 12 h, 1 d, 3 d, and 7 d after SAH. Afterward, the rats were anesthetized (*vide supra*) and 100 mL of saline at a temperature of 4 °C was perfused into the heart. Next, craniotomy was immediately performed and brain tissue obtained from the bilateral temporal lobe cortex and preserved at −80 °C until required for further analysis. For electron microscopy, the specimens were fixed in electron microscopy fixing solution at 4 °C for 24 h and sliced into ultrathin sections. For mRNA extraction, specimens were added to Trizol solution and preserved at −80 °C. Prior to tissue collection for frozen sections and paraffin embedding, animals were perfused with 4% paraformaldehyde.

#### 2.5. Western Blot Analysis

Tissue specimens were lysed and homogenized on ice, and then spun for 5 min at 10,000 rpm. A Millipore centrifugal filter and the Bradford assay were used to concentrate the samples and to measure the concentration of proteins in each sample, respectively. Equal quantities of protein were added to 4 × SDS buffer, incubated for 5 min at 95 °C, and then separated using SDS-PAGE. Samples were next transferred to PVDF membranes and blocked for 1 h at ambient room temperature, and then incubated overnight at 4 °C in the presence of an appropriate primary antibody. Next, the blots were exposed to horseradish peroxidase-conjugated secondary antibodies for 1 h. The primary antibodies were: anti-CIRP (1:500); anti-Bax; anti-Bcl-2 (1:200); anti-caspase-9; anti-caspase-3 (1:500); and anti-cytochrome c (1:5000). Horseradish peroxidase-coupled goat anti-rabbit secondary antibodies (1:5000) was then added for 1 h. After the detection of chemiluminescence, UN-Scan-It ver. 6.1 software was used for signal quantification.

For the detection of cytochrome c, cells were first snap-frozen on dry ice and then stored at −80 °C after which cytochrome c was purified by acid extraction at 4 °C [24]. Homogenates were centrifuged at 15,810 × *g* for 35 min, and then the supernatants were adjusted to pH 7.4 by adding KOH together with protease (1 mM PMSF) and phosphatase inhibitors (10 mM KF, 1 mM sodium orthovanadate). The supernatant samples were centrifuged after being subjected to ion exchange chromatography and run through a DE52 anion exchange column. Cytochrome c was present in the column outflow, which was adjusted to pH 6.5 and then run on a CM52 cation exchange column equilibrated with 30 mM phosphate buffer. The column bound cytochrome c was oxidized with 2 mM  $K_3Fe(CN)_6$  and eluted using step gradients of phosphate buffer at pH 6.5 (0, 50, 80, 120, and 150 mM). Pure fractions of cytochrome c were generated by repeating the above protocols, producing a mixture of phosphorylated and non-phosphorylated cytochrome c. Cytochrome c was vacuum-concentrated, desalted by centrifugation with Amicon Ultra-15 3 kDa centrifugal filter units, and stored at −80 °C until required for analysis.

#### 2.6. Expression Analysis of CIRP mRNA by Real-Time PCR

RNA was extracted from temporal cortex specimens using a Trizol kit. Reverse transcription was conducted using a kit from Toyobo and CIRP mRNA was measured by StepOne™ RT-PCR. The internal reference was GAPDH. The primers for CIRP were: 5'-GCTGGCAAGTCTTCTGATAACC-3' (forward); 5'-CGGCTGGCATAGTAGTCTCT-3' (reverse). The primers for GAPDH were: 5'-AGGTTGTCTCCTGTGACTTCAA-3' (forward); 5'-CTGTTGCTGTAGCCATATTCATTG-3' (reverse). Relative expression levels were evaluated by the  $2^{-\Delta\Delta C_t}$  method.

#### 2.7. Immunofluorescence Staining

One day after SAH, 7 μm-thick frozen sections of brain tissue from the coronal surface including the temporal cortex were produced as previously described [25]. Anti-NeuN (1:100, Millipore, Darmstadt, Germany) was used to stain neurons, whereas anti-GFAP

(1:200, Sigma, St. Louis, MO, USA) was used for astrocyte staining. Anti-CIRP was added at 1:200 and specimens were incubated in the dark overnight. Subsequently, samples were incubated in corresponding secondary antibodies for 2 h at ambient room temperature. DAPI was used to stain the nuclei and one drop of anti-fade mounting medium was added before the specimens were positioned on cover slips. Fluorescence images were captured on a Zeiss HB050 microscope.

### 2.8. TUNEL Staining

One day after SAH, 7  $\mu\text{m}$ -thick frozen sections of specimens from the coronal surface of the brain and temporal cortex were collected for TUNEL staining. TUNEL staining was performed using the Roche TUNEL kit. Brain sections were analyzed for apoptotic cells using a Fluorescence in Situ Cell Death Detection Kit, and the number of TUNEL-positive cells in areas surrounding a lesion was counted using ImageJ software.

Following exposure to the primary antibody overnight, slides were incubated with TUNEL reaction mixture at 37 °C for 1 h, washed several times with PBS and stained for 2 min with DAPI. The apoptosis rate was calculated using the equation:

$$\text{Apoptosis rate} = \frac{\text{the number of apoptotic cell}}{\text{total number of DAPI positive cells}}$$

### 2.9. Immunohistochemistry

Paraffin-embedded sections (4  $\mu\text{m}$ -thick) of brain tissue were acquired from the coronal surface of the brain 1 d after the SAH was stained. The sections were incubated overnight at 4 °C with a primary antibody against CIRP (1:200) and then washed for 15 min in PBS. Subsequently, they were incubated with horseradish peroxidase conjugated IgG at room temperature for 60 min. After a thorough wash, diaminobenzidine was applied as the chromogen and hematoxylin for counterstaining. Stained sections were examined under a light microscope at a magnification of  $\times 400$ .

### 2.10. Nissl Staining

Three days after SAH, Nissl staining was performed on 4  $\mu\text{m}$ -thick brain tissue sections taken from the coronal surface and embedded in paraffin. They were fixed in 100% methanol for 10 min, and rehydrated in a series of decreasing ethyl alcohol baths (95% 15 min, 70% 2 min, and 50% 2 min), rinsed twice with distilled water, and a cresyl violet stain applied for 6 min. Then, the sections were rinsed twice with distilled water for 2 min. Finally, the sections were dehydrated in a series of increasing ethyl alcohol baths (50% 2 min, 70% acidic ethyl alcohol 2 min, 95% 2 min, 95% a few immersions, and 100% 1 min). Histoclear was applied for 5 min to lighten the sections and slides were then cover-slipped in Histomount mounting media.

### 2.11. Cell Counting in Tissue Sections

Six fields of high-power ( $\times 400$ ) were randomly selected for each tissue section. Four sections in each rat and four rats in each group were selected for cell counting. In each field, the number or the percentage of positive cells were counted for statistical analyses.

### 2.12. Electron Microscopy

Ultrathin 70 nm sections of the temporal cortex were stretched with chloroform to eliminate compression and mounted on Pioloform filmed copper grids prior to staining with 2% aqueous uranyl acetate and lead citrate. The sections were viewed on a JEM-1011 transmission electron microscope to observe the morphology of mitochondria.

### 2.13. Rotarod Test

The motor functions of rats were assessed by the rotarod test as previously described [26]. Rats were trained on the rotarod for 3 d prior to an experiment. The exercise time, which is the time the animals remained on an accelerating rotarod cylinder, was

measured for each rat three times (>15 min intervals) per d before and 1, 3, and 7 d after SAH. The rotation rate was increased from 4 to 40 rpm over a 5 min time period.

2.14. Statistical Analysis

Statistical analyses were conducted using SPSS ver. 19.0. Measurement data that had a normal distribution are given as the mean ± SD. Data not following a normal distribution are presented as the median ± inter-quartile ranges. Enumeration data are reported as case numbers and percentages. A chi-squared test was employed to make comparisons of any differences in the rates between groups. The significance of differences in continuous variables between two groups was assessed with a nonparametric test or a *t*-test. Potential differences between multiple groups were evaluated using one-way ANOVA. A finding was deemed to be significant at a *p*-value < 0.05.

3. Results

3.1. Motor Functions of SAH Rats Undergoing Hypothermia Treatment Was Measured by the Rotarod Test

Compared to the Sham group, the SAH treatment reduced motor functions, with the most significant difference observed 24 h after SAH. Hypothermia treatment in the SAH + H group reduced the motor deficit (Figure 2A) in the first 3 d after SAH, but the motor functions had fully recovered after 7 d in all treatment groups.

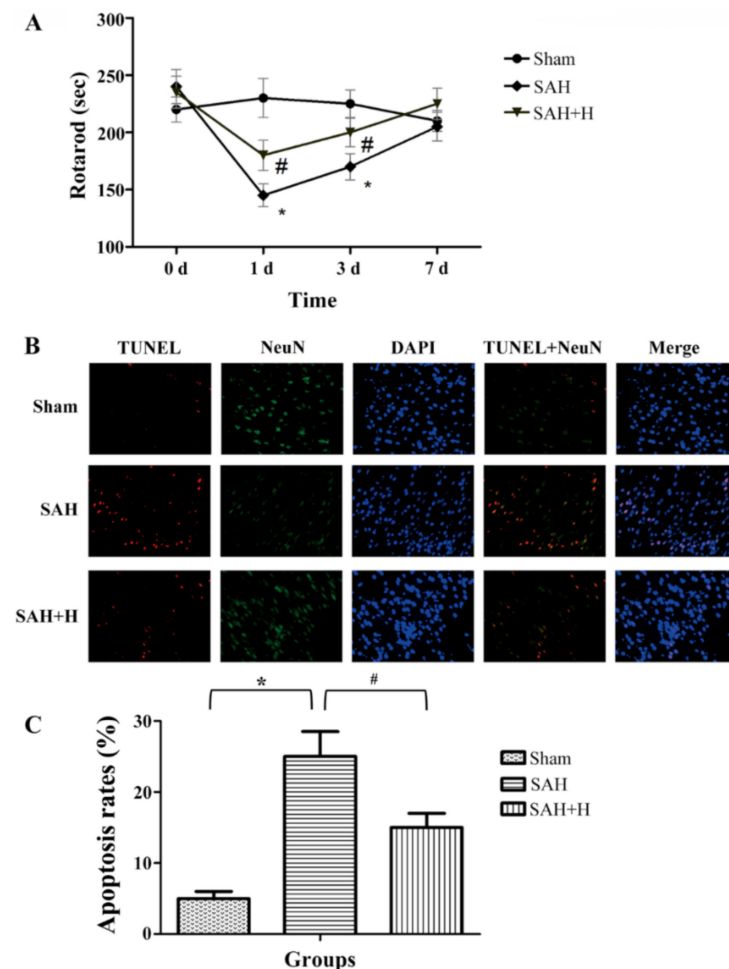


**Figure 2.** The rotarod and TUNEL staining. Rotarod test results (A) and TUNEL staining images (B) of the temporal cortexes for the indicated treatment groups (×400) 1 d after SAH induction. Panel (C) represents the apoptosis rates derived from the TUNEL assays. \* *p* < 0.05 SAH vs. Sham, # *p* < 0.05 SAH vs. SAH + H.

### 3.2. Protection of Neurons from SAH-Induced Apoptosis by Hypothermia Treatment

The SAH group showed marked apoptosis of neurons as revealed by TUNEL staining (Figure 2B,C) 1 d after the induction of SAH. However, hypothermia treatment significantly reduced the apoptosis of neuronal cells in the SAH + H group (Figure 2B,C), indicating that the hypothermia treatment had protected neurons from SAH injury.

### 3.3. Analysis of the Number of Surviving Neurons after Hypothermia Treatment

Nissl staining revealed a significant decrease in the number of surviving neurons after brain injury in the SAH compared to the Sham groups. Normal neurons have a large cell body and abundant cytoplasm with a large domed nucleus, while damaged neurons exhibited cell contraction as well as concentrated nuclear and cellular vacuoles. In contrast, hypothermia treatment increased the number of surviving neurons in the SAH + H group, demonstrating that cooling can effectively inhibit the damaging effects of SAH (Figure 3).

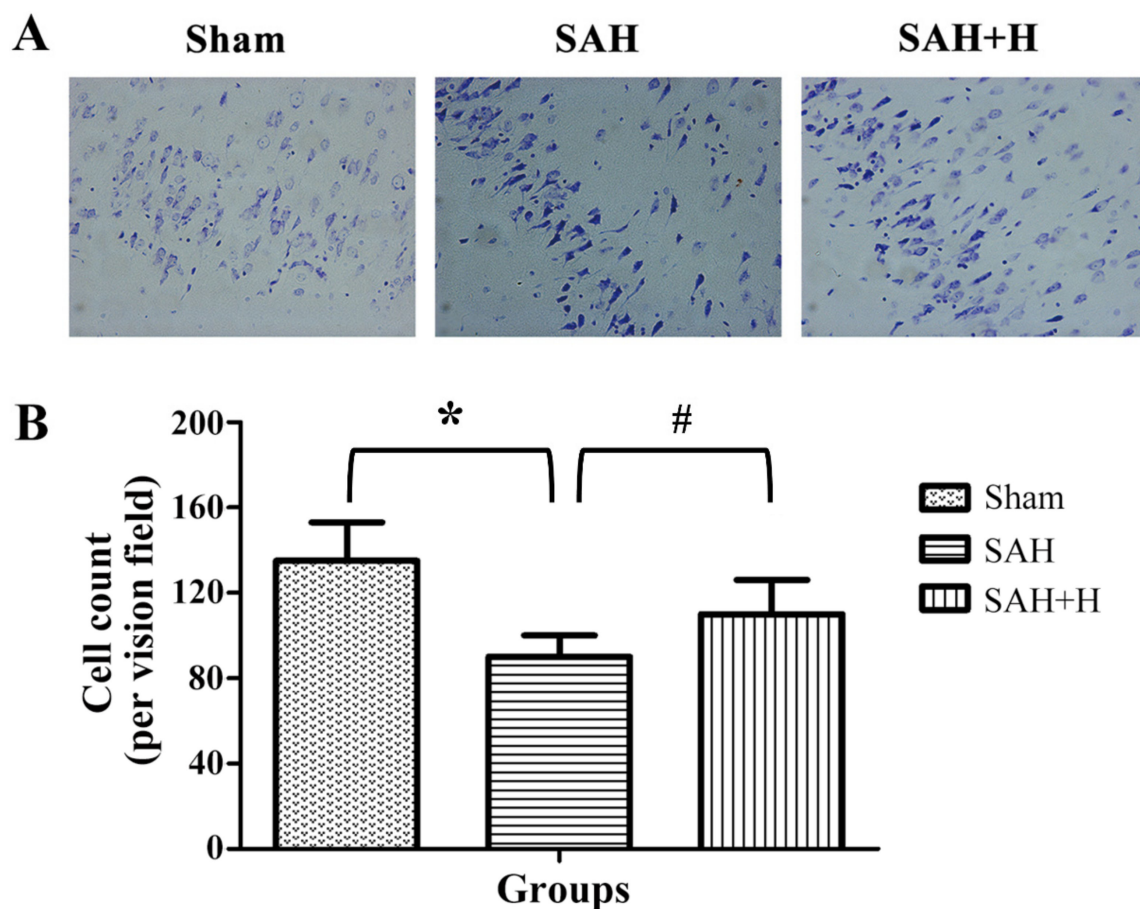


**Figure 3.** The Nissl staining of the temporal cortex paraffin sections 3 d after SAH. (A) Nissl staining images; (B) The numbers of surviving neurons as determined by microscopy ( $\times 400$ ) and cell counting. \*  $p < 0.05$  SAH vs. Sham, #  $p < 0.05$  SAH vs. SAH + H.

### 3.4. Distribution of CIRP in Rat Brain

Immunofluorescence staining showed that CIRP was mainly expressed in neurons and to some extent in astrocytes of brains from the SAH rats 1 d after the operation (Figure 4). Whole section images showed that CIRP was widely expressed in brain tissue including in the cerebral cortex and subcortical neurons. The distribution of astrocytes was distinctly different, showing signals in brain regions with fewer relationships to the CIRP expression level.

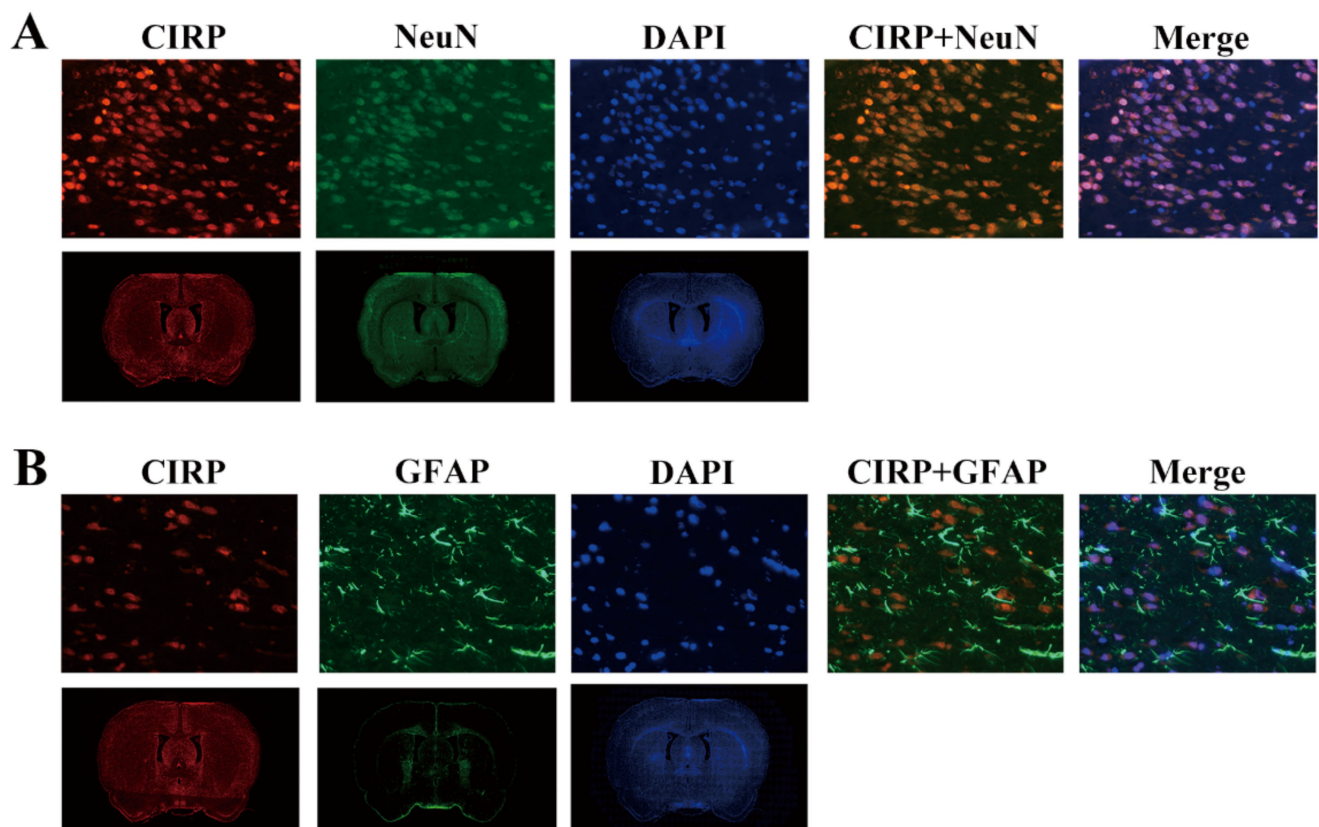


**Figure 4.** The distribution of CIRP in the rat brain tissue 1 d after SAH induction as determined by immunofluorescence staining. (A) Co-staining with NeuN; (B) Co-staining with GFAP. Micrographs in the top panels at a magnification of  $\times 400$ . Bottom panels show the whole cerebral coronal sections.

### 3.5. Analysis of CIRP mRNA and Protein Expression in the Temporal Cortex and Expression of Mitochondrial Apoptosis Pathway-Related Proteins

Immunohistochemical staining of the rat brain tissue revealed that hypothermia treatment in SAH rats significantly reduced the number of cells with CIRP staining (Figure 5A,B). Brain injury increased the expression of CIRP mRNA and protein at all time points examined in the SAH group, peaking 1 d after SAH. Compared to the SAH group, however, hypothermia ameliorated the SAH-induced transcription and expression levels of CIRP mRNA and protein 1, 3, and 7 d after SAH (Figure 5C–E). Moreover, the expression of Bax, caspase-9, and caspase-3 as well as the release of cytochrome c into the cytoplasm was increased in the brain after injury, whereas the expression of Bcl-2 at 12 h, 1 d, and 3 d was slightly decreased after SAH. In contrast, in the SAH + H group, induction of Bax, caspase-9, and caspase-3, and the secretion of cytochrome c were blunted, while the expression of Bcl-2 was greatly enhanced (Figure 5F–K). Transmission electron microscopy imaging revealed that the normal mitochondrial morphology observed in the Sham group was severely disturbed after SAH, with mitochondria displaying disintegration of the cristae structure and vacuolization (Figure 6). These morphological changes were attenuated by hypothermia treatment (Figure 6).



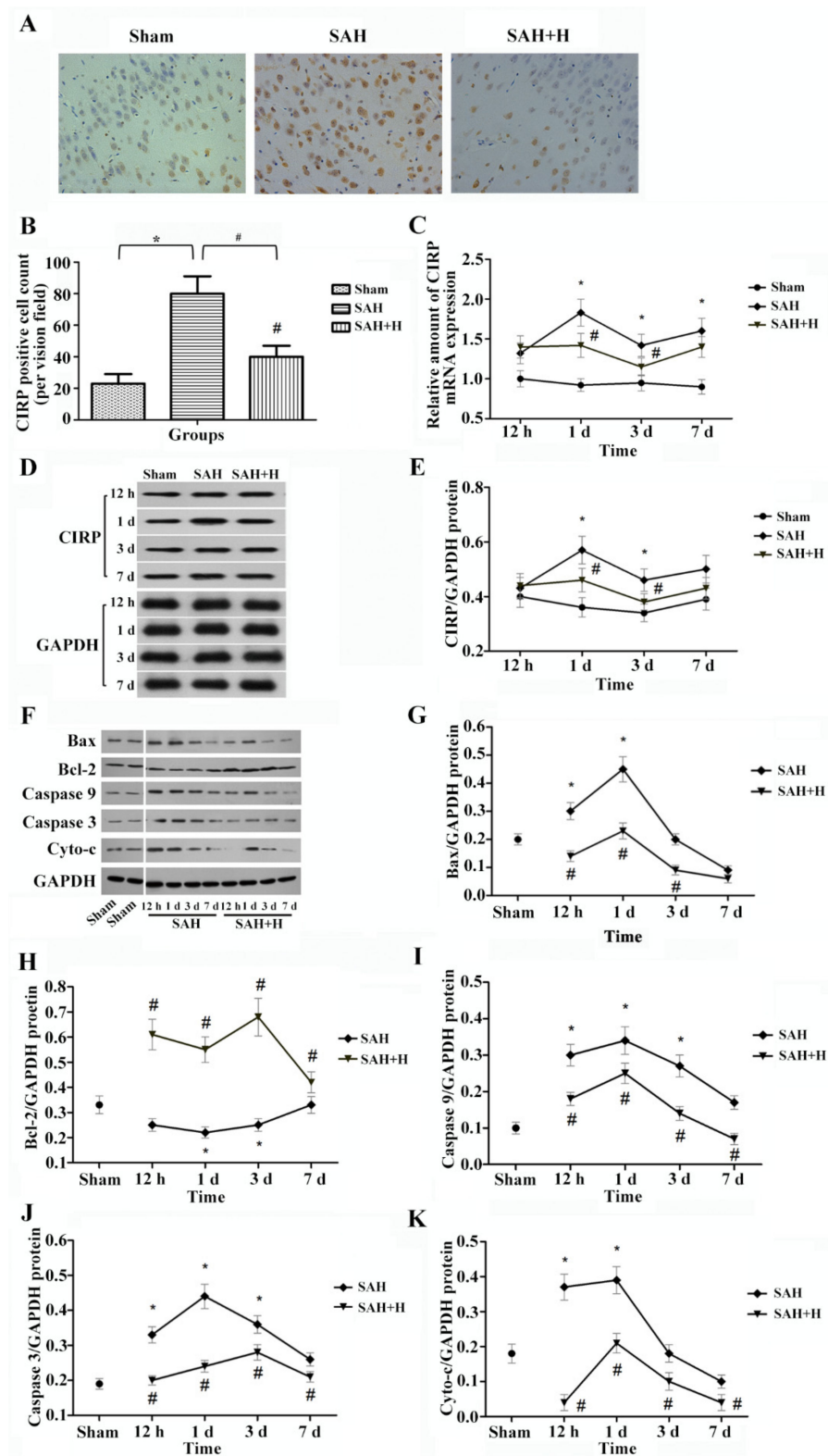


**Figure 5.** The analysis of CIRP mRNA and protein expression and mitochondrial apoptosis pathway-related proteins from 12 h to 7 d after SAH. (A,B) Immunohistochemical results of rat brain tissue ( $\times 400$ ) 1 d after SAH. (C–E) Expression levels of CIRP mRNA and protein at four time points. (C) Analysis of CIRP mRNA at four time points by RT-PCR. (D,E) Western blot analysis of the CIRP protein expression at four time points. (F–K) Expression of the mitochondrial apoptosis pathway-related proteins including Bax, Bcl-2, caspase-9, caspase-3, and cytochrome c. \*  $p < 0.05$  SAH vs. Sham; #  $p < 0.05$  SAH+H vs. SAH.

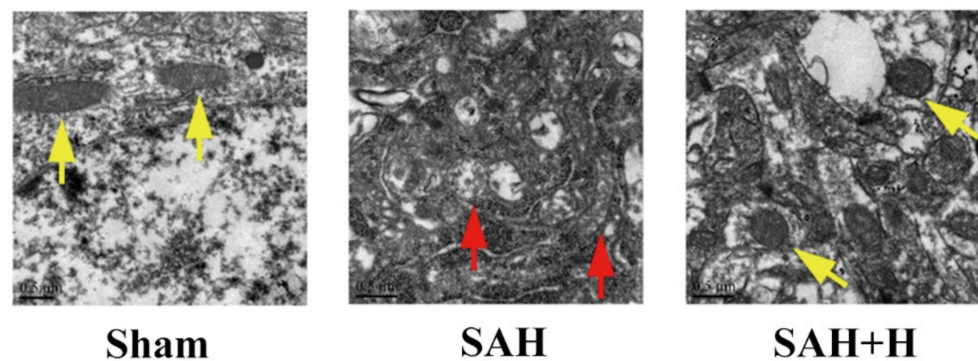


**Figure 6.** The transmission electron micrographs of neuronal mitochondria 1 d after SAH. Yellow arrows show normal mitochondrial morphology; red arrows point to abnormal mitochondrial morphology.

#### 4. Discussion

##### 4.1. Therapeutic Hypothermia Improved Motor Function and Decreased Mitochondrial Pro-Apoptotic Pathway Activation after SAH

In the SAH model, it was shown that therapeutic hypothermia reduced the motor function deficits of SAH rats, and effectively diminished the apoptosis of neurons in the early period after SAH operation. Therapeutic hypothermia also decreased the expression levels of pro-apoptotic proteins in the mitochondrial apoptosis pathway including Bax, caspase-9, and caspase-3. Hypothermia also reduced the secretion of cytochrome c into the cytoplasm and increased the expression of the anti-apoptotic protein Bcl-2. A previous study found that hypothermia could protect brain function by reducing the heat shock protein 70 expression mRNA in the cortex and hippocampus of SAH rats [27,28]. Schubert et al. demonstrated that hypothermia decreased cerebral edema and lactate accumulation in SAH rats to protect brain function [29]. Hypothermia was also reported to reduce the release of reactive oxygen species to protect neuronal functions [30]. In agreement with these previous reports, our study demonstrated that therapeutic hypothermia maintained the mitochondrial morphology of temporal cortex neurons, improved neuronal functions, and alleviated early brain injury induced by SAH.

##### 4.2. Alleviation of Early Brain Injury by Therapeutic Hypothermia Was Correlated with Decreased Expression of Pro-Inflammatory C1RP in the Cerebral Cortex of SAH Rats

Our study showed that the basal levels of C1RP are normally expressed in neurons, and that both hypothermia and SAH lead to increased neuronal C1RP expression. Mild hypothermia, osmotic stress, and hypoxia are known inducers of C1RP expression in cells [7,31]. C1RP is localized to the nucleus of human and rat cells under normal physiological conditions. However, it translocates to the cytoplasm and can be secreted when cells are subjected to environmental stress conditions [32]. Extracellular C1RP was reported to be a danger-associated molecular pattern (DAMP) with pro-inflammatory activity [33]. The concentration of C1RP in the blood increased in patients with hemorrhagic shock and was associated with a poor prognosis for sepsis [34,35]. Recombinant C1RP has been shown to stimulate the secretion of tumor necrosis factor- $\alpha$  (TNF- $\alpha$ ) and high-mobility group protein B1 from macrophages [14]. In addition, alcohol exposure induces the secretion of C1RP and possibly TNF- $\alpha$  and IL-1 $\beta$ , thereby causing neuroinflammation in the mouse brain [36]. Furthermore, the injection of anti-C1RP antibodies through the internal jugular vein markedly reduced inflammation and tissue damage in a hepatic ischemia-reperfusion model, thereby improving the viability of mice [37]. C1RP<sup>-/-</sup> mice exhibited an accelerated rate of wound healing [38]. Taken together, these reports are consistent with C1RP being a pro-inflammatory factor, which can induce an inflammatory response, leading to tissue damage. Suppression of C1RP expression and neuroinflammation may thus underlie the beneficial effects of hypothermia in the SAH model.

#### 4.3. Limitation of Animal Studies Regarding Long-Term Effects of SAH

In recent years, SAH research based on animal models has proposed the concept of early brain injury (EBI), that is, brain tissue injury is the most severe 1–3 d after modeling and has the greatest impact on the future prognosis, while 3–7 d after modeling, the brain tissue enters the recovery stage and has basically returned to normal at 7 d. One possible explanation is that in animal model studies of SAH, red blood cells and other metabolites were partially eliminated 3 days after modeling, while 3–7 d after modeling, the brain tissue enters the recovery stage and basically returned to normal at 7 d [22,39,40]. However, in the clinic, the brain injury of patients with SAH is still serious 7 d after hemorrhage. They may still show cerebral edema, headache, neck stiffness, and other symptoms, which in most patients will not be significantly improved until two to three weeks later [41,42]. Therefore, a limitation of the present study is that it cannot fully represent the clinical results of human SAH. In addition, another drawback of the present study is the limited sample size and the absence of a power analysis.

#### 5. Conclusions

The study confirmed that SAH significantly increased the expression of CIRP mRNA and protein in rats. In addition, the immunofluorescence staining experiments showed that all neurons expressed CIRP, leading to the widespread expression of CIRP in brain tissue. After hypothermia treatment, the expression levels of CIRP mRNA and protein in SAH rats were reduced in the early stage after SAH, also correlating with decreased cell apoptosis and improved motor functions in the early stage. Hypothermia reduced the expression of CIRP in the temporal cortex neurons, alleviated mitochondrial damage, and mitigated early brain injury following SAH.

**Author Contributions:** Conceptualization, H.D., Y.Z., J.M. and C.H.; Data curation, Z.Z., Y.G., G.L., C.C. and W.L.; Formal analysis, X.Z. and Y.L.; Validation, All authors; Visualization, All authors; Writing—original draft, H.D. and Y.Z.; Writing—review & editing, Y.L., X.Z., Z.Z., Y.G., G.L., C.C. and W.L. All authors have read and agreed to the published version of the manuscript.

**Funding:** This work was supported by the National Natural Science Foundation of China (NSFC) (grant numbers 82130037, 81971122, 81971127). The funder had no role in the design of the study or the collection, analysis, and interpretation of data or in writing the manuscript.

**Institutional Review Board Statement:** All of the experimental procedures were approved by the Animal Care and Use Committee of Nanjing University.

**Informed Consent Statement:** Not applicable.

**Data Availability Statement:** Not applicable.

**Conflicts of Interest:** The authors declare no conflict of interest.

#### References

1. Bederson, J.B.; Connolly, E.S., Jr.; Batjer, H.H.; Dacey, R.G.; Dion, J.E.; Diringer, M.N.; Duldner, J.E., Jr.; Harbaugh, R.E.; Patel, A.B.; Rosenwasser, R.H. Guidelines for the management of aneurysmal subarachnoid hemorrhage: A statement for healthcare professionals from a special writing group of the Stroke Council, American Heart Association. *Stroke* **2009**, *40*, 994–1025. [[CrossRef](#)]
2. Sehba, F.A.; Hou, J.; Pluta, R.M.; Zhang, J.H. The importance of early brain injury after subarachnoid hemorrhage. *Prog. Neurobiol.* **2012**, *97*, 14–37. [[CrossRef](#)]
3. Sehba, F.A.; Pluta, R.M.; Zhang, J.H. Metamorphosis of subarachnoid hemorrhage research: From delayed vasospasm to early brain injury. *Mol. Neurobiol.* **2011**, *43*, 27–40. [[CrossRef](#)] [[PubMed](#)]
4. Chowdhury, T.; Dash, H.H.; Cappellani, R.B.; Daya, J. Early brain injury and subarachnoid hemorrhage: Where are we at present? *Saudi J. Anaesth.* **2013**, *7*, 187–190. [[CrossRef](#)] [[PubMed](#)]
5. Fujii, M.; Yan, J.; Rolland, W.B.; Soejima, Y.; Caner, B.; Zhang, J.H. Early brain injury, an evolving frontier in subarachnoid hemorrhage research. *Transl. Stroke Res.* **2013**, *4*, 432–446. [[CrossRef](#)] [[PubMed](#)]
6. Soto-Cámara, R.; González-Santos, J.; González-Berna, J.; Trejo-Gabriel-Galán, J.M. Factors associated with a rapid call for assistance for patients with ischemic stroke. *Emergencias* **2020**, *32*, 33–39.
7. Liu, A.; Zhang, Z.; Li, A.; Xue, J. Effects of hypothermia and cerebral ischemia on cold-inducible RNA-binding protein mRNA expression in rat brain. *Brain Res.* **2010**, *1347*, 104–110. [[CrossRef](#)]

8. Wang, G.; Zhang, J.N.; Guo, J.K.; Cai, Y.; Sun, H.S.; Dong, K.; Wu, C.G. Neuroprotective effects of cold-inducible RNA-binding protein during mild hypothermia on traumatic brain injury. *Neural Regen. Res.* **2016**, *11*, 771–778. [[CrossRef](#)]
9. Xue, J.H.; Nonoguchi, K.; Fukumoto, M.; Sato, T.; Nishiyama, H.; Higashitsuji, H.; Itoh, K.; Fujita, J. Effects of ischemia and H<sub>2</sub>O<sub>2</sub> on the cold stress protein CIRP expression in rat neuronal cells. *Free Radic. Biol. Med.* **1999**, *27*, 1238–1244. [[CrossRef](#)]
10. Nishiyama, H.; Danno, S.; Kaneko, Y.; Itoh, K.; Yokoi, H.; Fukumoto, M.; Okuno, H.; Millán, J.L.; Matsuda, T.; Yoshida, O.; et al. Decreased expression of cold-inducible RNA-binding protein (CIRP) in male germ cells at elevated temperature. *Am. J. Pathol.* **1998**, *152*, 289–296.
11. Nishiyama, H.; Xue, J.H.; Sato, T.; Fukuyama, H.; Mizuno, N.; Houtani, T.; Sugimoto, T.; Fujita, J. Diurnal change of the cold-inducible RNA-binding protein (Circp) expression in mouse brain. *Biochem. Biophys. Res. Commun.* **1998**, *245*, 534–538. [[CrossRef](#)]
12. Fujita, J. Cold shock response in mammalian cells. *J. Mol. Microbiol. Biotechnol.* **1999**, *1*, 243–255.
13. Zhou, M.; Yang, W.L.; Ji, Y.; Qiang, X.; Wang, P. Cold-inducible RNA-binding protein mediates neuroinflammation in cerebral ischemia. *Biochim. Biophys. Acta* **2014**, *1840*, 2253–2261. [[CrossRef](#)]
14. Qiang, X.; Yang, W.L.; Wu, R.; Zhou, M.; Jacob, A.; Dong, W.; Kuncewitch, M.; Ji, Y.; Yang, H.; Wang, H.; et al. Cold-inducible RNA-binding protein (CIRP) triggers inflammatory responses in hemorrhagic shock and sepsis. *Nat. Med.* **2013**, *19*, 1489–1495. [[CrossRef](#)]
15. Lujan, D.A.; Ochoa, J.L.; Hartley, R.S. Cold-inducible RNA binding protein in cancer and inflammation. *Wiley Interdiscip. Rev. RNA* **2018**, *9*, e1462. [[CrossRef](#)]
16. Kollmar, R.; Juettler, E.; Huttner, H.B.; Dörfler, A.; Staykov, D.; Kallmuenzer, B.; Schmutzhard, E.; Schwab, S.; Broessner, G. Cooling in intracerebral hemorrhage (CINCH) trial: Protocol of a randomized German-Austrian clinical trial. *Int. J. Stroke* **2012**, *7*, 168–172. [[CrossRef](#)]
17. Van der Worp, H.B.; Sena, E.S.; Donnan, G.A.; Howells, D.W.; Macleod, M.R. Hypothermia in animal models of acute ischaemic stroke: A systematic review and meta-analysis. *Brain* **2007**, *130*, 3063–3074. [[CrossRef](#)]
18. Andresen, M.; Gazmuri, J.T.; Marín, A.; Regueira, T.; Rovegno, M. Therapeutic hypothermia for acute brain injuries. *Scand. J. Trauma Resusc. Emerg. Med.* **2015**, *23*, 42. [[CrossRef](#)]
19. Zhang, H.; Zhou, M.; Zhang, J.; Mei, Y.; Sun, S.; Tong, E. Therapeutic effect of post-ischemic hypothermia duration on cerebral ischemic injury. *Neurol. Res.* **2008**, *30*, 332–336. [[CrossRef](#)]
20. Legriell, S.; Lemiale, V.; Schenck, M.; Chelly, J.; Laurent, V.; Daviaud, F.; Srairi, M.; Hamdi, A.; Geri, G.; Rossignol, T.; et al. Hypothermia for Neuroprotection in Convulsive Status Epilepticus. *N. Engl. J. Med.* **2016**, *375*, 2457–2467. [[CrossRef](#)]
21. Wang, Q.; Zhang, L.; Yuan, X.; Ou, Y.; Zhu, X.; Cheng, Z.; Zhang, P.; Wu, X.; Meng, Y.; Zhang, L. The Relationship between the Bcl-2/Bax Proteins and the Mitochondria-Mediated Apoptosis Pathway in the Differentiation of Adipose-Derived Stromal Cells into Neurons. *PLoS ONE* **2016**, *11*, e0163327. [[CrossRef](#)] [[PubMed](#)]
22. Zhang, X.S.; Li, W.; Wu, Q.; Wu, L.Y.; Ye, Z.N.; Liu, J.P.; Zhuang, Z.; Zhou, M.L.; Zhang, X.; Hang, C.H. Resveratrol Attenuates Acute Inflammatory Injury in Experimental Subarachnoid Hemorrhage in Rats via Inhibition of TLR4 Pathway. *Int. J. Mol. Sci.* **2016**, *17*, 1331. [[CrossRef](#)] [[PubMed](#)]
23. Dai, H.B.; Xu, M.M.; Lv, J.; Ji, X.J.; Zhu, S.H.; Ma, R.M.; Miao, X.L.; Duan, M.L. Mild Hypothermia Combined with Hydrogen Sulfide Treatment During Resuscitation Reduces Hippocampal Neuron Apoptosis Via NR2A, NR2B, and PI3K-Akt Signaling in a Rat Model of Cerebral Ischemia-Reperfusion Injury. *Mol. Neurobiol.* **2016**, *53*, 4865–4873. [[CrossRef](#)] [[PubMed](#)]
24. Yu, H.; Lee, I.; Salomon, A.R.; Yu, K.; Hüttemann, M. Mammalian liver cytochrome c is tyrosine-48 phosphorylated in vivo, inhibiting mitochondrial respiration. *Biochim. Biophys. Acta* **2008**, *1777*, 1066–1071. [[CrossRef](#)]
25. Zhang, X.S.; Wu, Q.; Wu, L.Y.; Ye, Z.N.; Jiang, T.W.; Li, W.; Zhuang, Z.; Zhou, M.L.; Zhang, X.; Hang, C.H. Sirtuin 1 activation protects against early brain injury after experimental subarachnoid hemorrhage in rats. *Cell Death Dis.* **2016**, *7*, e2416. [[CrossRef](#)]
26. Chen, G.; Zhang, S.; Shi, J.; Ai, J.; Qi, M.; Hang, C. Simvastatin reduces secondary brain injury caused by cortical contusion in rats: Possible involvement of TLR4/NF-kappaB pathway. *Exp. Neurol.* **2009**, *216*, 398–406. [[CrossRef](#)]
27. Kawamura, Y.; Yamada, K.; Masago, A.; Katano, H.; Matsumoto, T.; Mase, M. Hypothermia modulates induction of hsp70 and c-jun mRNA in the rat brain after subarachnoid hemorrhage. *J. Neurotrauma* **2000**, *17*, 243–250. [[CrossRef](#)]
28. Török, E.; Klopotoski, M.; Trabold, R.; Thal, S.C.; Plesnila, N.; Schöller, K. Mild hypothermia (33 degrees C) reduces intracranial hypertension and improves functional outcome after subarachnoid hemorrhage in rats. *Neurosurgery* **2009**, *65*, 352–359, discussion 359. [[CrossRef](#)]
29. Schubert, G.A.; Poli, S.; Schilling, L.; Heiland, S.; Thomé, C. Hypothermia reduces cytotoxic edema and metabolic alterations during the acute phase of massive SAH: A diffusion-weighted imaging and spectroscopy study in rats. *J. Neurotrauma* **2008**, *25*, 841–852. [[CrossRef](#)]
30. Lv, O.; Zhou, F.; Zheng, Y.; Li, Q.; Wang, J.; Zhu, Y. Mild hypothermia protects against early brain injury in rats following subarachnoid hemorrhage via the TrkB/ERK/CREB signaling pathway. *Mol. Med. Rep.* **2016**, *14*, 3901–3907. [[CrossRef](#)]
31. Pan, F.; Zarate, J.; Choudhury, A.; Rupperecht, R.; Bradley, T.M. Osmotic stress of salmon stimulates upregulation of a cold inducible RNA binding protein (CIRP) similar to that of mammals and amphibians. *Biochimie* **2004**, *86*, 451–461. [[CrossRef](#)]
32. De Leeuw, F.; Zhang, T.; Wauquier, C.; Huez, G.; Kruys, V.; Gueydan, C. The cold-inducible RNA-binding protein migrates from the nucleus to cytoplasmic stress granules by a methylation-dependent mechanism and acts as a translational repressor. *Exp. Cell Res.* **2007**, *313*, 4130–4144. [[CrossRef](#)]

33. Aziz, M.; Brenner, M.; Wang, P. Extracellular CIRP (eCIRP) and inflammation. *J. Leukoc. Biol.* **2019**, *106*, 133–146. [[CrossRef](#)]
34. Chen, K.; Cagliani, J.; Aziz, M.; Tan, C.; Brenner, M.; Wang, P. Extracellular CIRP activates STING to exacerbate hemorrhagic shock. *JCI Insight* **2021**, *6*, e143715. [[CrossRef](#)]
35. Zhou, Y.; Dong, H.; Zhong, Y.; Huang, J.; Lv, J.; Li, J. The Cold-Inducible RNA-Binding Protein (CIRP) Level in Peripheral Blood Predicts Sepsis Outcome. *PLoS ONE* **2015**, *10*, e0137721. [[CrossRef](#)]
36. Rajayer, S.R.; Jacob, A.; Yang, W.L.; Zhou, M.; Chaung, W.; Wang, P. Cold-inducible RNA-binding protein is an important mediator of alcohol-induced brain inflammation. *PLoS ONE* **2013**, *8*, e79430. [[CrossRef](#)]
37. Godwin, A.; Yang, W.L.; Sharma, A.; Khader, A.; Wang, Z.; Zhang, F.; Nicastrò, J.; Coppa, G.F.; Wang, P. Blocking cold-inducible RNA-binding protein protects liver from ischemia-reperfusion injury. *Shock* **2015**, *43*, 24–30. [[CrossRef](#)]
38. Idrovo, J.P.; Jacob, A.; Yang, W.L.; Wang, Z.; Yen, H.T.; Nicastrò, J.; Coppa, G.F.; Wang, P. A deficiency in cold-inducible RNA-binding protein accelerates the inflammation phase and improves wound healing. *Int. J. Mol. Med.* **2016**, *37*, 423–428. [[CrossRef](#)]
39. Shao, J.; Wu, Q.; Lv, S.Y.; Zhou, X.M.; Zhang, X.S.; Wen, L.L.; Xue, J.; Zhang, X. Allicin attenuates early brain injury after experimental subarachnoid hemorrhage in rats. *J. Clin. Neurosci.* **2019**, *63*, 202–208. [[CrossRef](#)]
40. Xia, D.Y.; Zhang, H.S.; Wu, L.Y.; Zhang, X.S.; Zhou, M.L.; Hang, C.H. Pentoxifylline Alleviates Early Brain Injury After Experimental Subarachnoid Hemorrhage in Rats: Possibly via Inhibiting TLR 4/NF- $\kappa$ B Signaling Pathway. *Neurochem. Res.* **2017**, *42*, 963–974. [[CrossRef](#)]
41. Liu, J.P.; Ye, Z.N.; Lv, S.Y.; Zhuang, Z.; Zhang, X.S.; Zhang, X.; Wu, W.; Mao, L.; Lu, Y.; Wu, L.Y.; et al. The rise of soluble platelet-derived growth factor receptor  $\beta$  in CSF early after subarachnoid hemorrhage correlates with cerebral vasospasm. *Neurol. Sci.* **2018**, *39*, 1105–1111. [[CrossRef](#)]
42. Lv, S.Y.; Wu, Q.; Liu, J.P.; Shao, J.; Wen, L.L.; Xue, J.; Zhang, X.S.; Zhang, Q.R.; Zhang, X. Levels of Interleukin-1 $\beta$ , Interleukin-18, and Tumor Necrosis Factor- $\alpha$  in Cerebrospinal Fluid of Aneurysmal Subarachnoid Hemorrhage Patients May Be Predictors of Early Brain Injury and Clinical Prognosis. *World Neurosurg.* **2018**, *111*, e362–e373. [[CrossRef](#)]